

Deep learning Gravitational Wave Detection in the Frequency Domain

Juan Pablo Marulanda², Camilo Santa², and Antonio Enea Romano^{1,2}

¹*Theoretical Physics Department, CERN,
CH-1211 Geneva 23, Switzerland*

²*ICRANet, Piazza della Repubblica 10,
I65122 Pescara, Italy*

(Dated: April 3, 2020)

Detection of gravitational waves (GW) from compact binary mergers provide a new window into multimessenger astrophysics. The standard technique to determine the merger parameters is matched filtering, consisting in comparing the signal to a template bank. This approach can be time consuming and computationally expensive due to the large amount of experimental data which needs to be analyzed.

In the attempt to find more efficient data analysis methods we develop a new frequency domain convolutional neural network (FCNN) to predict the merger masses from the spectrogram of the detector signal, and compare it to previous time domain neural networks (TCNN). Since FCNNs are trained using spectrograms, the dimension of the input is reduced as compared to TCNNs, implying a substantially lower number of model parameters, consequently allowing faster processing, and a better out of sample performance. We find that in general FCNN have better performance on validation data and lower over-fit, providing a new promising approach to the analysis of GW detectors data.

Introduction According to general relativity, gravitational waves propagate at the speed of light and in the linear perturbative regime are produced by the second order time derivative of the quadrupole moment. The main sources of gravitational waves that can be detected at the Laser Interferometer Gravitational Wave Observatory (LIGO) and Virgo collaborations are the mergers of compact binary systems composed by black holes or neutron stars.

Due to the no-hair theorem, the merger of two black holes has no electromagnetic counterpart [1] but binary star mergers can have electromagnetic signals, therefore opening a new window into multi-messenger astronomy. These systems are known as standard sirens because the gravitational wave signal provides information of the distance to the objects independent of the cosmic distance ladder and their electromagnetic counterparts provide information about their speed. Therefore, they can be used to measure the Hubble parameter [1, 2] or to constrain alternative gravity theories with superluminal or subluminal GW speeds [3].

In order to achieve this goal, the detectors must have a strain sensitivity of the order of $10^{-21}/\sqrt{Hz}$ [4] and the standard data analysis approach consist in using matched filtering to compare the detector signal to a bank of gravitational wave templates in order to determine the merger parameters. Neural networks can be used to denoise the raw signal [5, 6] as a preprocessing step before matched filtering. This data analysis process must be repeated for every signal, which can be very time consuming and computationally expensive depending on the size of the template bank. Another approach has been developed [7–15] in which the time domain detector data is processed by a convolu-

tional neural network to predict the merger masses. In this paper we present the results of applying CNN to the frequency domain data, i.e. the Fourier transform of the time domain data, and call these neural networks FCNN, to distinguish them from the CNN applied to time domain data, which we denote as TCNN.

The FCNN relies on the short-time Fourier transform to extract the frequency domain features needed to train the network. This approach allows to reduce the dimensionality of the input, and the FCNN has in fact about 70.000 parameters, compared with almost 500.000 of the TCNN. As a direct consequence FCNN have better out of sample performance compared to TCNN, and tend to also have a lower over-fit, due to the significantly lower number of parameters.

Training Data generation The training data is generated using the package PyCBC[16], developed by the LIGO and Virgo collaborations.

This library contains a method to generate the waveform corresponding to a GW event, and accepts as inputs several different parameters [17]. In the waveform generation we assumed for simplicity the spins and orbital eccentricities to be zero, as in [7]. Data with $\pi/2$ polarization were also generated in order to see how the neural network would perform with signals with different parameters. The networks were trained to predict the two masses of the merger, while other parameters were kept fixed in the data generation. We choose the other parameters using the default values of the waveform generator function `get_td_waveform` except for the following parameters : the approximant is chosen to be the fourth version of Spin Effective One Body Numerical Relativity (SEOBNR) due to its efficiency, the sampling rate is 4096 Hz and the starting frequency is 20Hz.

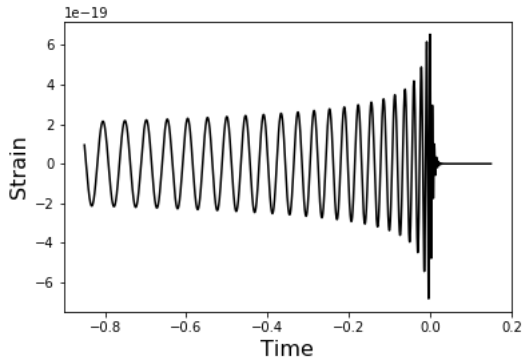


FIG. 1: Simulated strain of a black hole merger with 20 and 60 solar masses sampled at 4096Hz.

In order to train the networks with realistic data we add noise to the simulated signal. Before adding noise, the GW signal was first shifted temporally by a random shift in the interval $[0, 0.2]$ seconds, and the last second of the shifted signal was used for training, similarly to [7], in order to make the model more robust. We generated data with different signal-to-noise ratios (SNR), and colored noise was added according to the power spectral density (PSD) provided by LIGO. An example of the signal and the corresponding noised signal is shown in fig.(2).

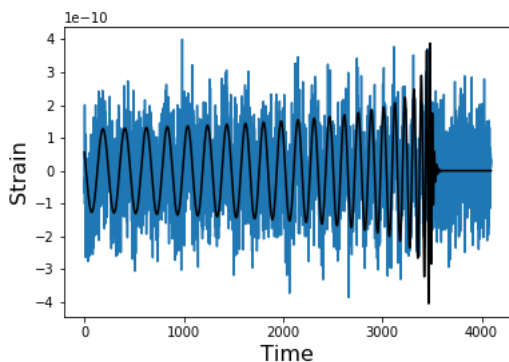


FIG. 2: Simulated data with colored noise sampled from a PSD provided by LIGO. Original clean signal is the solid black line while the signal with added noise is blue.

We train the the CNN using spectrograms, which are two dimensional matrices whose columns are related to the frequency power spectra of the strain ST at different times, according to

$$SP_{\omega} = 10 * \log_{10}(|ST_{\omega}|^2) \quad (1)$$

where SP_{ω} is the spectrogram, and ST_{ω} is the Fourier transform of the ST over different time intervals.

The spectrograms are obtained by performing a Fast Fourier Transform (FFT) using equally spaced time

intervals, with sampling frequency of 4096 Hz, windows of 128 elements, and an overlap between windows of 64 elements.

The spectrograms of a clean and noised signal are shown in fig.(3) and fig.(4), where it can be seen that the merger is mainly noticeable at low frequencies. As a consequence, for the purpose of training the CNN the spectrogram can be cropped, using as input only the lower half, since there is where the information of the merger is mostly located.

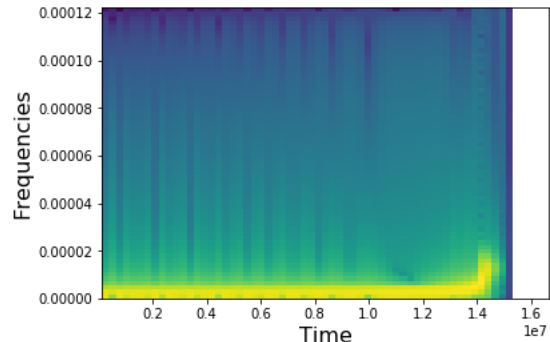


FIG. 3: Spectrogram of a clean signal of a binary black hole merger with 20 and 60 solar masses. The colors correspond to the values of the spectrogram from 200 (dark blue) to 150 (yellow).

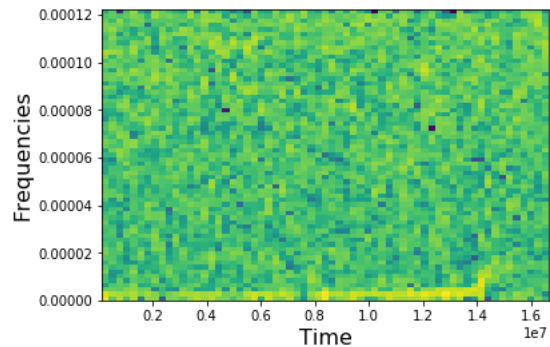


FIG. 4: Spectrogram of a colored signal of a binary black hole merger with 20 and 60 solar masses and SNR=0.1.

CNN architectures The TCNN described in [7], summarized in Table I, was implemented as a benchmark to compare the performance of the FCNN to.

The FCNN, whose architecture is shown in Table II, consists of three convolutional layers that perform 2D convolutions on the zero-padded signal, followed by a max pooling layer. The resulting output of the pooling layer is then flattened into a one dimensional vector of 512 entries, which is fed into a two layer fully connected net, that predicts the two masses of the merger.

The FCNN has about 70.000 parameters, compared with almost 500.000 of the TCNN. The smaller num-

ber of parameters reduces the variance of the model, making it less prone to over-fitting as the number of degrees of freedom is greatly reduced. This is achieved because the spectrogram reduces the total number of input components, the number of convolutions is less than the TCNN and the two dimensional pooling operation reduces the number of components more than the one dimensional pooling.

	Layer	Size
	Input	vector (4096)
1	Convolution (ReLU)	matrix (4096 × 16)
2	Pooling	matrix (1024 × 16)
3	Convolution(ReLU)	matrix (1024 × 32)
4	Pooling	matrix (256 × 32)
5	Convolution (ReLU)	matrix (256 × 64)
6	Flatten	vector(16384)
7	Dense layer (ReLU)	vector (64)
	Output	vector (2)

TABLE I: Architecture of the TCNN used in [7].

	Layer	Size
	Input	matrix (31 × 63 × 1)
1	Convolution (ReLU)	matrix (31 × 63 × 16)
2	Convolution (ReLU)	matrix (31 × 63 × 8)
3	Convolution (ReLU)	matrix (31 × 63 × 4)
4	Pooling	matrix (8 × 16 × 4)
5	Flatten	vector(512)
6	Dense layer (ReLU)	vector (32)
7	Dense layer (ReLU)	vector (16)
	Output	vector (2)

TABLE II: Architecture of the FCNN.

Over-fit When the training set error is very low, due to a high number of parameters, there is a risk over-fitting, which manifests in a large difference between the training and validation errors. In fact, even if the error of the model on the training set reaches low values, it does not necessarily imply that its predictive ability when applied on data different from the training set will be as good. In order to quantify the difference between the training and the validation errors we define the following over-fitting estimator:

$$O = \left| \frac{\text{train error} - \text{test error}}{\text{test error}} \right| \quad (2)$$

The lower the over-fit is, the smaller the generalization error of the model is, and therefore the out of sample data performance improves.

Regressor model The purpose of this model is to predict the masses of the merger from the spectrogram of the gravitational wave's strain signal. We train the

model by minimizing in each epoch the mean absolute percentage error (MAPE), defined as

$$MAPE = \frac{1}{n} \sum_{i=1}^n \sum_{j=1}^2 \left| \frac{\hat{M}_{ij} - M_{ij}}{M_{ij}} \right| \quad (3)$$

where n is the number of samples in each epoch, \hat{M}_{i1} and \hat{M}_{i2} are the masses of the merger predicted by the model, while M_{i1} and M_{i2} are the masses from the training set used in the simulation for the $i - th$ sample.

Training The model was trained for 1000 epochs, with simulated data generated for mass values from $10M_{\odot}$ to $75M_{\odot}$, and a mass pair ratio less than 5. A total of 4139 mergers with a SNR of 0.1 were simulated, dividing the simulated data in two subsets, a 70% training set, and a 30% validation set. The values the masses of the simulated mergers is shown in fig.(5).

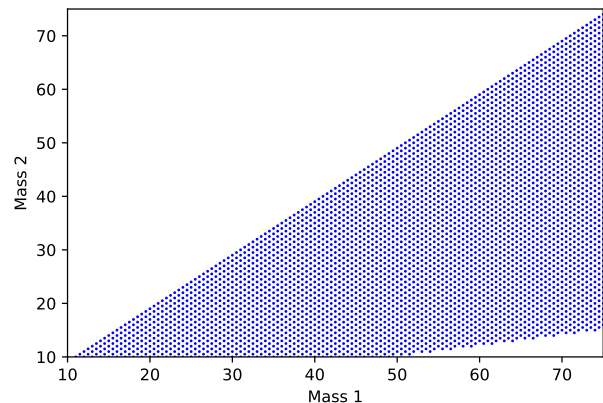


FIG. 5: Scatter plot of the mass pairs used to generate the simulated data on which the neural networks are trained and validated.

The training and validation errors of the predicted merger masses for FCNN and TCNN with zero polarization are shown in fig.(6) and fig.(7).

These figures show that the TCNN developed in [7] performs well during training, reaching a lower error than FCNN, but the latter has a better performance on the validation set, as confirmed by the lower over-fit estimator shown in fig.(8).

In fig.(8) the over-fit of the two models is shown, as defined in eq.(2). As mentioned earlier, the FCNN has much fewer parameters than TCNN, and it is therefore expected to have a lower over-fit than TCNN. In order to test the robustness of the models under the change of other merger parameters we also created another set training and validation data, using a different polarization angle. Gravitational wave signals with a polarization angle of $\pi/2$ were simulated keeping all other parameters fixed. We used the same

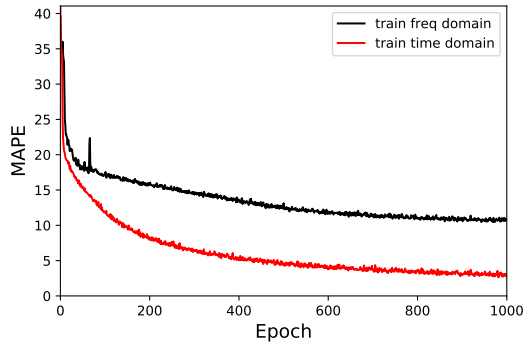


FIG. 6: The MAPEs of the TCNN and FCNN models are plotted as a function of the epochs, using a training data set with SNR = 0.1, and polarization = 0.

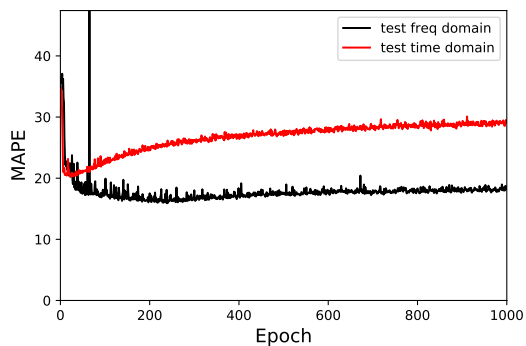


FIG. 7: The MAPEs of the TCNN and FCNN models are plotted as a function of the epochs, using a validation data set with SNR = 0.1, and polarization = 0.

number of simulated samples, and the masses of the mergers ranged from $10M_{\odot}$ to $75M_{\odot}$ with a mass ratio less than or equal to 5.

The training and validation error of the TCNN and FCNN models for data with $\pi/2$ polarization is shown in fig.(9) and fig.(10) respectively. Similarly to the models trained with zero polarization simulated data, the TCNN model performed better on the training data, but the FCNN has a lower error than the TCNN on the validation set.

The over-fit of TCNN models for simulated data with $\pi/2$ polarization is shown in fig.(11). The FCNN over-fit was lower than for TCNN, suggesting that FCNN generalizes better than TCNN also on signals from gravitational waves with different parameters.

Conclusions We have developed a new convolutional neural network, FCNN, to determine the masses of mergers, trained on the spectrograms of the signal of simulated GW signals, and compared its performance with other CNN trained on time domain data (TCNN) [7].

The networks were trained for 1000 epochs using 4139 merger signals with a 70-30 training/validation split, and the cost function which was minimised was

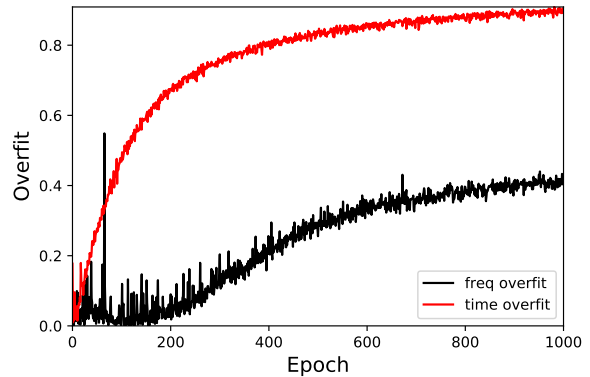


FIG. 8: The over-fit of the TCNN and FCNN models is plotted as a function of the epochs, using a data set with SNR = 0.1, and polarization = 0.

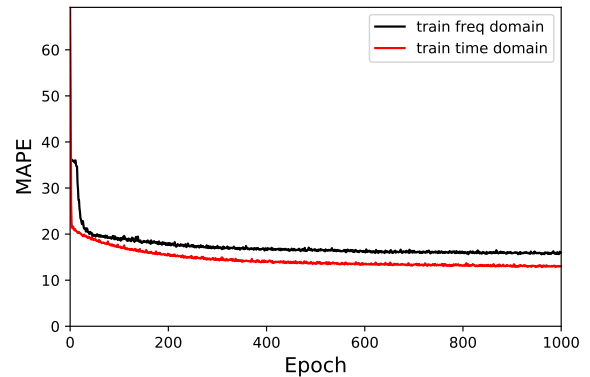


FIG. 9: The MAPEs of the TCNN and FCNN models are plotted as a function of the epochs, using a training data set with SNR = 0.1, and polarization = $\pi/2$.

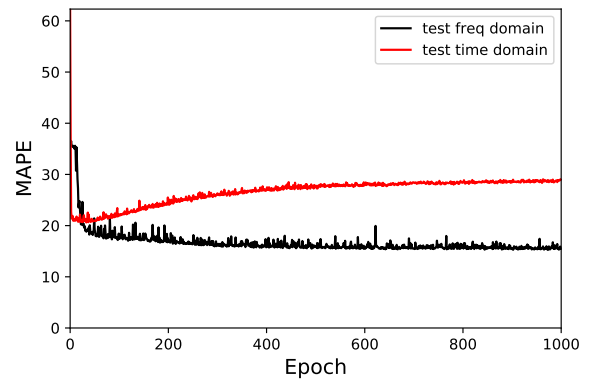


FIG. 10: The MAPEs of the TCNN and FCNN models are plotted as a function of the epochs, using a validation data set with SNR = 0.1, and polarization = $\pi/2$.

the sum of mean absolute percentage errors between the masses and their predictions.

The FCNN is trained on spectrograms, allowing to reduce the dimension of the input, implying also a lower number of parameters in the final fully con-

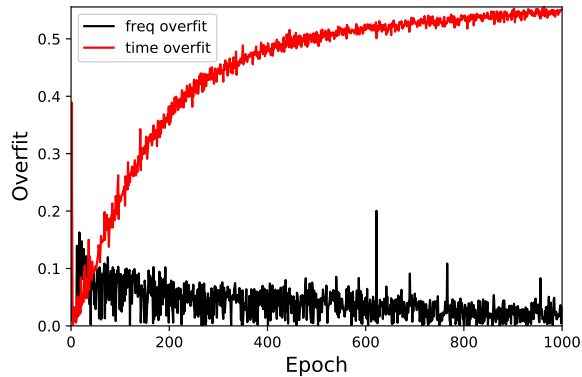


FIG. 11: The over-fit of the TCNN and FCNN models is plotted as a function of the epochs, using a data set with $\text{SNR} = 0.1$, and polarization $= \pi/2$.

nected layers of the network, and reducing its variance. The total amount of floating point operations also decreases and the network can perform inference much faster. FCNN have better out of sample performance compared to TCNN, and tend to also have a lower over-fit, due to the significantly lower number of parameters.

In the future it will be interesting to design more complex FCNN in order to predict additional parameters such as the spins and orbital eccentricities, or to apply it to data simulated for other detectors such as the Laser Interferometer Space Antenna.

[1] LIGO Scientific, Virgo, B. P. Abbott *et al.*, (2019), arXiv:1908.06060.

- [2] B. F. Schutz, *Nature* **323**, 310 (1986).
- [3] LIGO Scientific, Virgo, Fermi-GBM, INTEGRAL, B. P. Abbott *et al.*, *Astrophys. J.* **848**, L13 (2017), arXiv:1710.05834.
- [4] B. P. Abbott *et al.*, *Phys. Rev.* **D93**, 112004 (2016), arXiv:1604.00439, [Addendum: *Phys. Rev. D* **97**, no.5, 059901 (2018)].
- [5] H. Shen, D. George, E. A. Huerta, and Z. Zhao, (2017), arXiv:1711.09919.
- [6] W. Wei and E. A. Huerta, *Phys. Lett.* **B800**, 135081 (2020), arXiv:1901.00869.
- [7] D. George and E. A. Huerta, *Phys. Rev.* **D97**, 044039 (2018), arXiv:1701.00008.
- [8] D. George and E. A. Huerta, *Phys. Lett.* **B778**, 64 (2018), arXiv:1711.03121.
- [9] D. George and E. A. Huerta, Deep Learning for Real-time Gravitational Wave Detection and Parameter Estimation with LIGO Data, in *NiPS Summer School 2017 Gubbio, Perugia, Italy, June 30-July 3, 2017*, 2017, arXiv:1711.07966.
- [10] A. Rebei *et al.*, *Phys. Rev.* **D100**, 044025 (2019), arXiv:1807.09787.
- [11] H. Gabbard, M. Williams, F. Hayes, and C. Messenger, *Phys. Rev. Lett.* **120**, 141103 (2018), arXiv:1712.06041.
- [12] X. Fan, J. Li, X. Li, Y. Zhong, and J. Cao, *Sci. China Phys. Mech. Astron.* **62**, 969512 (2019), arXiv:1811.01380.
- [13] J. A. Gonzalez and F. S. Guzman, *Phys. Rev.* **D97**, 063001 (2018), arXiv:1803.06060.
- [14] A. J. K. Chua, C. R. Galley, and M. Vallisneri, *Phys. Rev. Lett.* **122**, 211101 (2019), arXiv:1811.05491.
- [15] H. Nakano *et al.*, *Phys. Rev.* **D99**, 124032 (2019), arXiv:1811.06443.
- [16] Visit <https://pycbc.org/> for more info.
- [17] For a full list of these parameters, visit https://pycbc.org/pycbc/latest/html/_modules/pycbc/waveform/parameters.html